LA-UR - 78 - 1335

TITLE: NUMERICAL STUDIES OF MULTIPHASE FLOW IN A PRESSURIZED WATER REACTOR

AUTHOR(S): B. J. Daly

SUBMITTED TO: International Seminar on Momentum, Heat and Mass Transfer in Two Phase Energy and Chemical Systems (ICHMT)
Belgrade, Yugoslavia
4-9 September 1978

By acceptance of this article for publication, the publisher recognizes the Government's (license) rights in any copyright and the Government and its authorized representatives have unrestricted right to reproduce in whole or in part said article under any copyright secured by the publisher.

The Los Alamos Scientific Laboratory requests that the publisher identify this article as work performed under the auspices of the USERDA.

los alamos
scientific laboratory
of the University of California
LOS ALAMOS, NEW MEXICO 87545

An Affirmative Action/Equal Opportunity Employer

NOTICE
This report was prepared as an account of work sponsored by the United States Government. Neither the United States nor the United States Department of Energy, nor any of their employees, nor any of their contractors, subcontractors, or their employees, makes any warranty, express or implied, or assumes any legal liability or responsibility for the accuracy, completeness or usefulness of any information, apparatus, product or process disclosed, or represents that its use would not infringe privately owned rights.

Form No. 836
St. No. 2629
1/75

UNITED STATES
ENERGY RESEARCH AND
DEVELOPMENT ADMINISTRATION
CONTRACT W-7405-ENG. 36

DISTRIBUTION OF THIS DOCUMENT IS UNLIMITED

NUMERICAL STUDIES OF MULTIPHASE FLOW IN A PRESSURIZED WATER REACTOR

BART J. DALY
Group T-3, Theoretical Division
University of California
Los Alamos Scientific Laboratory
Los Alamos, NM 87545

ABSTRACT

The K-TIF numerical method for calculating the transient dynamics of two interpenetrating fluids has been extended and applied to the study of flow in a pressurized water reactor during a hypothetical loss of coolant accident. The method is verified by the comparison of results with small scale experiments. The extension to larger scale provides a tentative prediction of the appropriate inflow velocity scaling required to achieve flow similarity at all scales.

INTRODUCTION

An area of interest in nuclear reactor safety studies is the hypothetical accident in which a sudden depressurization of a pressurized water reactor (PWR) occurs through the rupture of a water inlet supply pipe. As a result of such a hypothetical depressurization the coolant water in the reactor core would flash to steam and flow toward the broken inlet leg. In the unlikely event of a loss of coolant accident of this type, an emergency water supply is injected through the intact inlet legs into the downcomer, which is the annular region between the reactor core and the outer vessel wall. The effectiveness of the emergency core coolant depends upon the amount that reaches the lower plenum of the reactor; any coolant that is entrained by the rising steam flow and carried out the broken leg will be lost to the system.

In this study we examine the turbulent mixing of the liquid and gas phases in this downcomer region, and the resulting mass, momentum and heat transfer between the phases and the confining walls. Solutions are obtained through the use of the K-TIF numerical method [1] for calculating the transient dynamics of two interpenetrating fluids moving at far subsonic speeds. Mass and momentum equations for the liquid and the gas and a temperature equation for the liquid are solved in this numerical procedure. The gas is always assumed to be at saturation temperature. The capability exists for subdividing the gas phase into two components, steam and air, in order to account for the possible introduction of air to the system if the downcomer pressure falls below ambient.

The numerical method is verified by a comparison of calculated results with experimental measurements in scale models of existing PWR's for a variety of water injection rates and subcoolings, steam flow and pressure ramp rates and wall superheat. The numerical method is also used to calculate flow at scales larger than existing experimental models and at full scale. These scaling studies have a threefold purpose: to provide guidance for PWR licensing, to aid in the interpretation of small scale experiments, and to help assess the potential usefulness of proposed large scale experimental facilities.

THE PHYSICAL MODEL

The flow model described here is an extension of that proposed by Amsden and Harlow [1]. The reader is referred to that reference for a more detailed description.

It is assumed in this study that sound velocity is much greater than material velocity so that microscopic density is independent of position. However, the effect of temporal variations in gas density as a result of overall compression or expansion of the fluid is included. With these considerations, the mass conservation equations can be written

$$\frac{\partial \psi_1}{\partial t} + \nabla \cdot (\psi_1 \vec{u}_1) = - J/\rho_1 - S_1 \quad , \tag{1}$$

$$\frac{\partial \psi_2}{\partial t} + \nabla \cdot (\psi_2 \vec{u}_2) = + J/\rho_2 - S_2 - \frac{\psi_2}{\rho_2} \frac{d\rho_2}{dt} \quad . \tag{2}$$

The subscripts 1 and 2 refer to water and gas, respectively; ψ is volume fraction, $\vec{u}$ is velocity, ρ is microscopic density, J is the mass per unit volume per unit time changing phase and S is the volume per unit volume per unit time entering or leaving the system.

The steam is assumed to be always at the saturation temperature, T_s. Accordingly, the phase change model is written

$$J = J_L \psi_{eff} (T_1 - T_s)/T_s \quad , \tag{3}$$

where T is temperature and

$$\psi_{eff} = \begin{cases} \psi_1 \text{ if } T_1 > T_s \text{ (evaporation)} \\ \psi_1 \psi_2 \alpha \text{ if } T_1 < T_s \text{ (condensation)} \end{cases} \tag{4}$$

Here α is the fraction of the gas volume that is steam, the remainder being air. The form for ψ_{eff} reflects the fact that evaporation can take place in the absence of steam (there being an abundance of nucleation sites in this turbulently mixed flow), but that condensation requires the movement of cool water to the phase transition interface where water and steam exist in equilibrium. Condensation then takes place to the extent allowed by the release of latent heat and the consequent heating of the water. We assume that the gas components are sufficiently well mixed through turbulence that the available steam can come into contact with the water.

The coefficient J_L in Eq. (3) is a negative constant in the calculations reported here, but an anticipated extension is to relate J_L to the magnitude of the local turbulent mixing rate.

Air can enter the system through the broken water supply pipe if the pressure in the downcomer drops below the external pressure as a result of condensation in the downcomer. This air is then convected throughout the downcomer and lower plenum with the gas velocity. Its presence can affect condensation locally by occupying volume that would otherwise be occupied by steam. However, in the highly mixed, turbulent flow that we are considering, it is assumed that the air does not obstruct the contact surface between steam and water.

The momentum equations for this two-phase flow are written

$$\frac{\partial(\psi_1\vec{u}_1)}{\partial t} + \nabla\cdot(\psi_1\vec{u}_1\vec{u}_1) = -\frac{\psi_1}{\rho_1}\nabla p + \psi_1\vec{g} + \frac{K}{\rho_1}(\vec{u}_2 - \vec{u}_1) + \nu_{T1}(\nabla\cdot\psi_1\nabla)\vec{u}_1 - \frac{J}{2\rho_1}\left[(1 + \text{sign } J)\,\vec{u}_1 + (1 - \text{sign } J)\,\vec{u}_2\right] , \quad (5)$$

$$\frac{\partial(\psi_2\vec{u}_2)}{\partial t} + \nabla\cdot(\psi_2\vec{u}_2\vec{u}_2) = -\frac{\psi_2}{\rho_2}\nabla p + \psi_2\vec{g} + \frac{K}{\rho_2}(\vec{u}_1 - \vec{u}_2) + \nu_{T2}(\nabla\cdot\psi_2\nabla)\vec{u}_2 + \frac{J}{2\rho_2}\left[(1 + \text{sign } J)\,\vec{u}_1 + (1 - \text{sign } J)\,\vec{u}_2\right] - \frac{\psi_2\vec{u}_2}{\rho_2}\frac{d\rho_2}{dt} , \quad (6)$$

where p is the pressure, $\vec{g}$ is the gravitational acceleration, ν_T is the kinematic eddy viscosity coefficient and

$$\text{sign } J = \begin{cases} +1 \text{ for } J > 0 \\ -1 \text{ for } J < 0 \end{cases} .$$

The momentum exchange function K has the form

$$K = \frac{3}{8}(r_1 + r_2)^2\left(\frac{C_D\rho_1\psi_1\rho_2\psi_2}{r_1 r_2}\right)\left(\frac{|\vec{u}_1 - \vec{u}_2|}{r_2\rho_1 + r_1\rho_2}\right) , \quad (7)$$

where r is entity size and C_D is the drag coefficient. If $\psi_2 < 0.1$, K is set to a large value with the effect that the gas then moves with the liquid. With this provision the k formulation in Eq. (7) reduces to the appropriate limits for small ψ_1 and small ψ_2, and is intended to be appropriate for intermediate values. This momentum exchange function was proposed by Harlow and Amsden [2] on the basis of available momentum arguments. It has previously been applied in comparisons with countercurrent air-water experiments [3]. A discussion of the choice of entity size is presented in the following section.

With the assumption that the steam is always at saturation temperature, only a transport equation for water temperature is required,

$$\frac{\partial T_1\psi_1}{\partial t} + \nabla\cdot(T_1\psi_1\vec{u}_1) + \frac{JT_s}{\rho_1} = -\frac{Q}{\rho_1 b_1}J + \frac{z\,k_w\,(T_{dw} - T_s)}{\rho_1\,b_1\,s\gamma} . \quad (8)$$

Here Q is the specific latent heat of vaporization, b_1 is the specific heat of the water, z is the number of walls adjacent to the water, k_w is the thermal conductivity of the wall, T_{dw} is the deep interior wall temperature, s is the downcomer gap width and γ measures the depth of penetration of a heating or cooling wave into the wall. We assume in Eq. (8) that the wall edge is at saturation temperature when water is adjacent to the wall. The presence of the downcomer gap width, s, in the denominator of the heat flux term in Eq. (8) ensures that the effect of wall heat flux is diminished as the system scale size is increased.

An equation for the depth of penetration, γ, is obtained by assuming that a solution to the wall heat diffusion equation,

$$\frac{\partial T_w}{\partial t} + K_w \frac{\partial^2 T_w}{\partial \xi^2} = 0 \quad , \tag{9}$$

can be expressed in terms of the similarity function,

$$\eta = \xi / \left(2 \sqrt{K_w t}\right) . \tag{10}$$

Here, T_w is the wall temperature, ξ is distance from the wall edge and K_w is the thermometric conductivity. The solution to Eq. (9), subject to the appropriate boundary conditions, is

$$T_w = T_{dw} + (T_s - T_{dw}) \left[1 - \frac{2}{\sqrt{\pi}} \operatorname{erf}(\eta)\right] . \tag{11}$$

We choose γ to be that value of ξ at which $T_w = .9\, T_{dw} + .1\, T_s$. This occurs when $\eta \approx 1.0$ or $\gamma = 2\sqrt{K_w t}$. From this we obtain an equation for the time variation of γ^2,

$$\frac{\partial \gamma^2}{\partial t} = 4K_w \quad . \tag{12}$$

CHARACTERISTIC ENTITY SIZE

Some guidance regarding the variation of entity size with scale can be obtained from empirical counter-current air-water flow correlations and the balance of forces concepts upon which they are based. At equilibrium, the balance between buoyancy and drag forces acting over a single spherical drop can be written,

$$C_D \; 1/2 \; \rho_2 \; (\vec{u}_1 - \vec{u}_2)^2 \; \pi r^2 = |\vec{g}| \; (\rho_1 - \rho_2) \; 4/3 \; \pi r^3 \quad ,$$

where r is the drop radius. If the average drop velocity is zero, the dimensionful quantities can be grouped to give

$$\frac{\rho_2 \, u_2^2}{|\vec{g}| \; 2r(\rho_1 - \rho_2)} = \frac{4}{3C_D} \quad , \tag{13}$$

where $\vec{u}_2$ is the minimum gas velocity required to prevent water penetration. The Wallis [4] and Kutateladze [4] correlations for zero water penetration differ in the manner of modeling the droplet diameter, 2r. Richter and Lovell [4] found, when this entity size was assumed to scale in proportion to the pipe size, that the left hand side of Eq. (13) remained approximately constant for pipes with diameters less than two inches. This is the Wallis correlation. However, this correlation breaks down at a larger pipes sizes, indicating a limit to the importance of boundary effects on entity size.

For pipe sizes larger than 2 inches they found that the zero penetration data could best be correlated by using the Kutateladze correlation,

$$2r = \left[\frac{\sigma}{g(\rho_1 - \rho_2)}\right]^{\frac{1}{2}} = 0.11 \text{ in. for air-water,} \tag{14}$$

where σ is the surface tension coefficient. This form can be obtained by balancing surface tension and drag forces and using Eq. (13). Then

$$r^2 = 3/8\ C_D\ We\ \frac{\sigma}{g(\rho_1 - \rho_2)} \quad , \tag{15}$$

where We is the Weber number for an isolated drop. Equations (14) and (15) are equivalent when $C_D We = 0.67$. In the numerical study we obtain the best agreement with experiment when $C_D = 0.6$, so that $We = 1.1$ is consistent with the Kutateladze entity size expression. Indeed, in the numerical calculations we have found that the use of a critical Weber number formulation for r, $r = We \times \sigma/[\rho_2(\vec{u}_1-\vec{u}_2)^2]$, with $We = 1.1$, or the use of a constant value, $r = 0.06$ in. [in good agreement with Eq. (14)], gives the best and essentially the same results.

Substituting Eq. (14) into Eq. (13), one can obtain the form of the Kutateladze correlation,

$$\frac{\rho_2^{1/2}|\vec{u}_2|}{[g\ \sigma(\rho_1 - \rho_2)]^{1/2}} = \left(\frac{8}{3}\frac{We}{C_D}\right)^{1/2} \quad . \tag{16}$$

Evaluating the right hand side of Eq. (16) with the values used in the numerical calculations gives a value of 1.5. In the Kutateladze correlation for pipes the value of the right hand side of Eq. (16) is generally found to be approximately 3.0 [4]. This quantitative discrepancy is quite acceptable in view of the differences in geometry between calculation and experiment as well as the heuristic arguments leading to Eq. (16).

APPLICATION OF THE METHOD

A. Comparisons with 1/15 and 2/15-Scale Models of a PWR

The K-TIF code has been used to calculate a series of transient steam-water flows [5] for comparison with specific experiments [6] performed by Creare, Inc. in a 1/15th scale model of a pressurized water reactor. A comparison of the calculated and experimental measurements of the time delay and rate of delivery of water from the downcomer to the lower plenum showed a consistent trend for a variety of water injection rates and subcoolings, steam flow and pressure ramp rates and wall superheat. In all cases the numerical calculations predicted a shorter delay time for the onset of water delivery to the lower plenum than was measured in the experiments.

The K-TIF model used in that comparison has since been extended by several modifications (e.g., the inclusion of an air component in the gas field and a more local determination of the momentum exchange function, K) that tend to prolong the delay time for water delivery. This extended version of K-TIF has been used to simulate a transient flow experiment performed in a 2/15 scale model of a PWR by Battelle Columbus Laboratories [7]. Figure 1 shows the computation mesh used in that numerical calculation. For display purposes the downcomer annulus is pictured as unwrapped. In the calculations the flow is resolved in the azimuthal (horizontal) and vertical directions, but flow variations across the downcomer gap are not resolved. The left and right boundaries of the mesh are connected while the top is a free-slip boundary. The bottom is a prescribed inflow boundary for the time-varying steam flow from the lower plenum and a continuative outflow boundary for the water and the gas. The deep lower plenum used in the experiment is not resolved in the calculations.

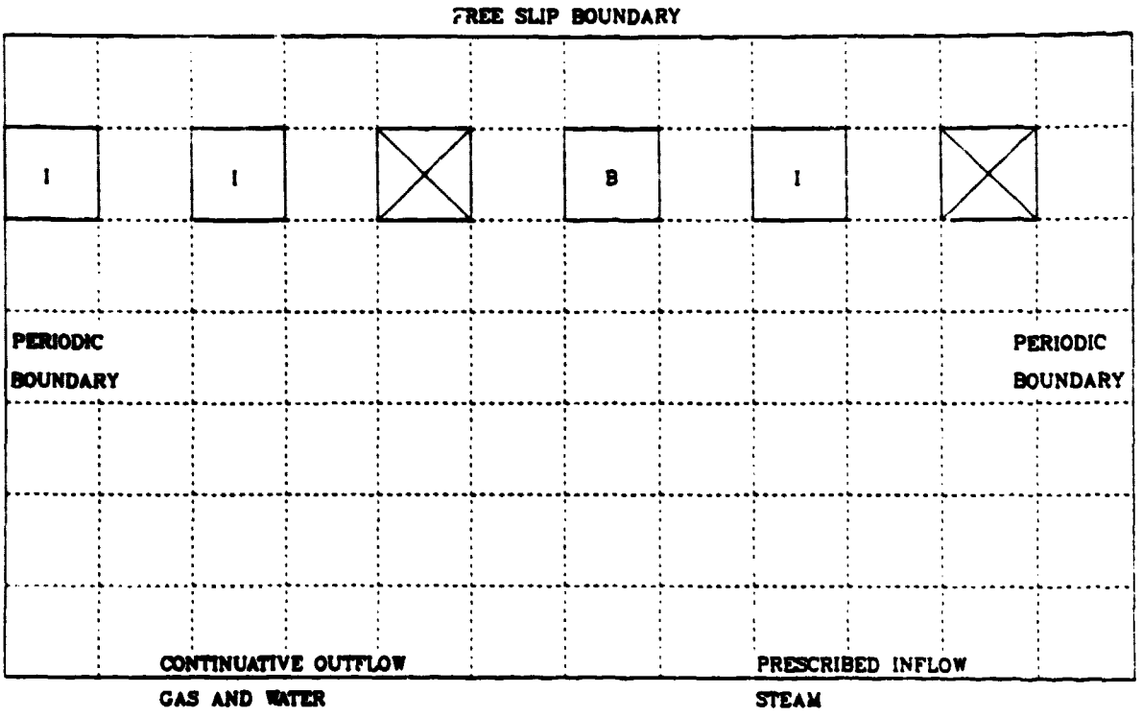

Fig. 1. Computation mesh and boundary conditions used in flow comparison with 2/15 scale experiment by Battelle Columbus Laboratories. The cells labeled I near the top of the mesh represent intact inlet pipes for coolant water. The cell labeled B represents a broken inlet pipe.

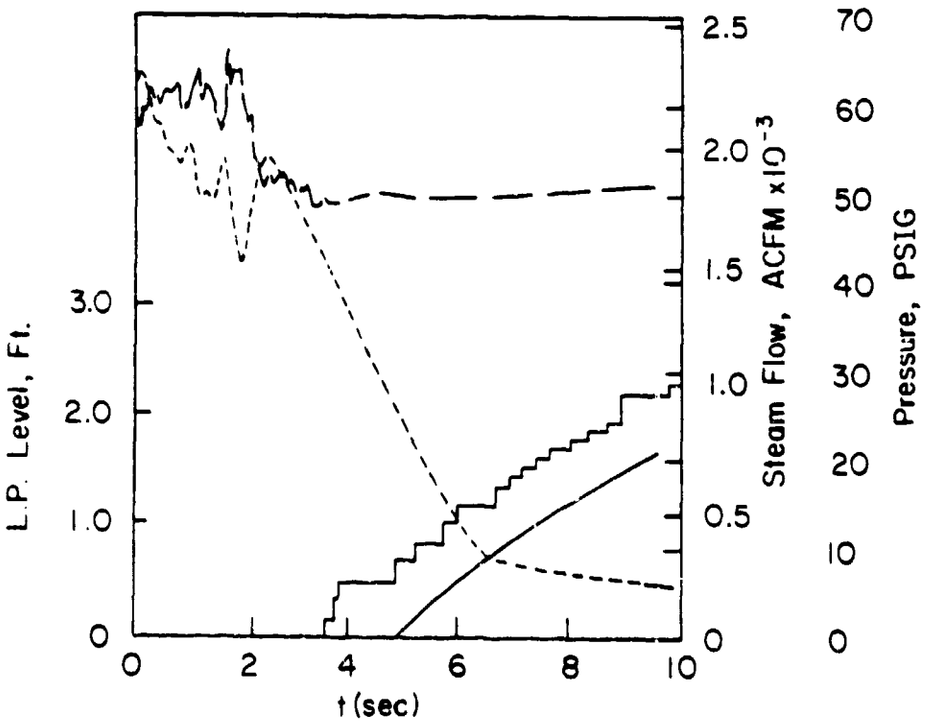

Fig. 2. The transient steam flow (---) and lower plenum pressure (— —) measured by Battelle Columbus Laboratories in a 2/15 scale model experiment, representing a hypothetical loss of coolant accident in a PWR.

Emergency core coolant enters the downcomer through the three intact cold water injection ports, labeled I, near the top of the mesh. Water and gas (steam and air) can leave the downcomer through the broken cold water pipe, labeled B. However, if the pressure in the downcomer falls below ambient as a result of condensation, so that there is flow into the downcomer through the broken leg, then the fluid flowing into the system is air. The two cross-hatched mesh cells near the top of the mesh simulate hot water pipes connecting the reactor core with the external power generating equipment. These are treated as obstacles in the numerical calculation.

In the Battelle experiment, 168°F (93°K) subcooled water is injected at the rate of 407 gallons (1541 liters) per minute through the three intact cold legs. The time-varying steam flow and lower plenum pressure are shown in Fig. 2. The core barrel and vessel walls are at the initial saturation temperature, 303°F (424°K).

The numerical calculation of this experiment makes use of a computation grid of square cells, 6.05 inches on a side, with 12 cells in the horizontal direction and 7 cells in the vertical direction. The water injection rate corresponds to that of the experiment, but the steam flow ramp rate and the pressure transient used in the calculation are smooth representations of the curves shown in Fig. 2.

Figure 2 also shows a comparison of the measured and calculated lower plenum filling curves as they vary in time. The experimental liquid level is measured at discrete sensing positions, giving rise to a stair-step appearance to the curve. The calculated liquid level is obtained by computing the total volume of water crossing the bottom boundary of the downcomer and dividing by the cross sectional area of the lower plenum. The two curves are in satisfactory agreement regarding the delay time for the onset of water delivery to the lower plenum, and in good agreement regarding the rate of delivery.

B. Sensitivity to Apparatus Scale Size

A series of K-TIF calculations has been performed in order to investigate the sensitivity of the flow dynamics at different apparatus scales to the water and steam inflow boundary condition scaling. It should be emphasized that the results to be presented here are preliminary and that much additional work remains to be done before a full understanding of flow variations with apparatus scale is obtained. The tentative nature of the present results derives from several considerations:

1. The lack of flow representation in the radial direction, the consequences of which could vary with scale.
2. Uncertainties regarding the constitutive relations. For example, the mass exchange function, Eq. (3), does not take into account the turbulent nature of the flow in the downcomer, which must have an important effect upon the details of interphase mixing. The momentum exchange function, Eq. (7), is novel and has not yet been sufficiently tested for simpler flow conditions.
3. While the flow model described here has been shown to give results that are consistent with small scale experiments for many flow conditions [4], quantitative agreement has not yet been demonstrated for a wide spectrum of flow variations.
4. Some of the parameter variations considered in the following study have not previously been tested in small scale comparisons.

With these reservations in mind, let us examine the trends indicated in these numerical calculations regarding the effects of various inflow scaling formulas on the similarity of flow development at 2/15, 1/2, and full scales. We shall describe flow similarity at different scales according to two criteria:

1. Agreement in the per cent of injected water that has been delivered to the lower plenum when the lower plenum is 90% full. This is an important criterion since it measures the effectiveness of the emergency core coolant supply system at full scale. The ultimate usefulness of small scale experiments rests on their ability to accurately predict the percentage.

2. Close similarity in fluid configuration at the onset of water delivery to the lower plenum. It has been observed in these calculations that the distribution and dynamics of water flow in the downcomer develops in three stages, as illustrated in Fig. 3. In the initial stage the water that is injected into the downcomer accumulates as single large entities, or "globs." This water is then entrained in the second stage by the upward directed steam flow and set in a swirling motion in the region above the inlet legs. Because of a favorable pressure gradient, part of this swirling water escapes from (bypasses) the system through the broken inlet leg. In the final stage of flow development, sufficient water accumulates below the intact cold legs that momentum transfer from the steam produces bypass from below the broken leg.

Depending on the inflow conditions, some flows may not proceed beyond the first or the second stage of this development. For example, if the water injection rate is small the local overpressure resulting from the inflow will not be large. Hence there will be little spreading of the water interface, so that the area of contact between the phases will remain small and little momentum transfer will take place unless the steam flow rate is large. The water will then fall into the lower plenum as two isolated streams below the injection legs. With somewhat more spreading or increased steam flow the momentum transfer may be sufficient to give rise to the swirling flow development. Delivery to the lower plenum then occurs as a single, rapidly falling water stream. As the momentum transfer is increased even more, bypass may occur from below the broken leg as indicated in Fig. 3. The increased contact area between the phases results in increased momentum transfer through condensation and interfacial drag. Water delivery to the lower plenum is thereby delayed.

The second criterion that we have used in defining flow similarity is that the flows must have reached the same stage of flow development before the onset of water delivery to the lower plenum. The reasonableness of this criterion for flow similarity rests on the observation that the timing and nature of flow delivery from the downcomer to the lower plenum varies greatly depending upon the stage of flow development that has been reached. Therefore, if small scale experiments are to be an accurate representation of full scale events, it would appear to be important that the two flows have reached the same stage of flow development prior to delivery to the lower plenum.

Calculations were performed at 2/15, 1/2, and full scales using the calculation mesh shown in Fig. 4. In these calculations the lower plenum is explicitly resolved as a linear extension of the downcomer with the appropriate volume. Boundary conditions are identical to those described for Fig. 1, except that steam is now injected throughout the entire lower plenum rather than being prescribed at the boundary between the downcomer and the lower plenum, and the bottom boundary condition now represents a free-slip rigid wall.

The lower plenum pressure, which is used to determine the gas density and saturation temperature, was ramped from 175 psia to 60 psia in 10 seconds and then held constant in all calculations. The steam injection velocity, which corresponds to the volume rate of flow into the downcomer divided by its cross sectional area, is linearly rampled from an initial value to zero in 10 seconds. The water injection velocity, determined from the volume rate of flow through three inlet legs divided by the cross sectional area of the downcomer, is a specified constant throughout any calculation.

Figures 5-8 show plots of water delivered to the lower plenum and bypassed through the broken leg as percentages of the total water injected up to that time for various types of inflow boundary specification. The results shown at

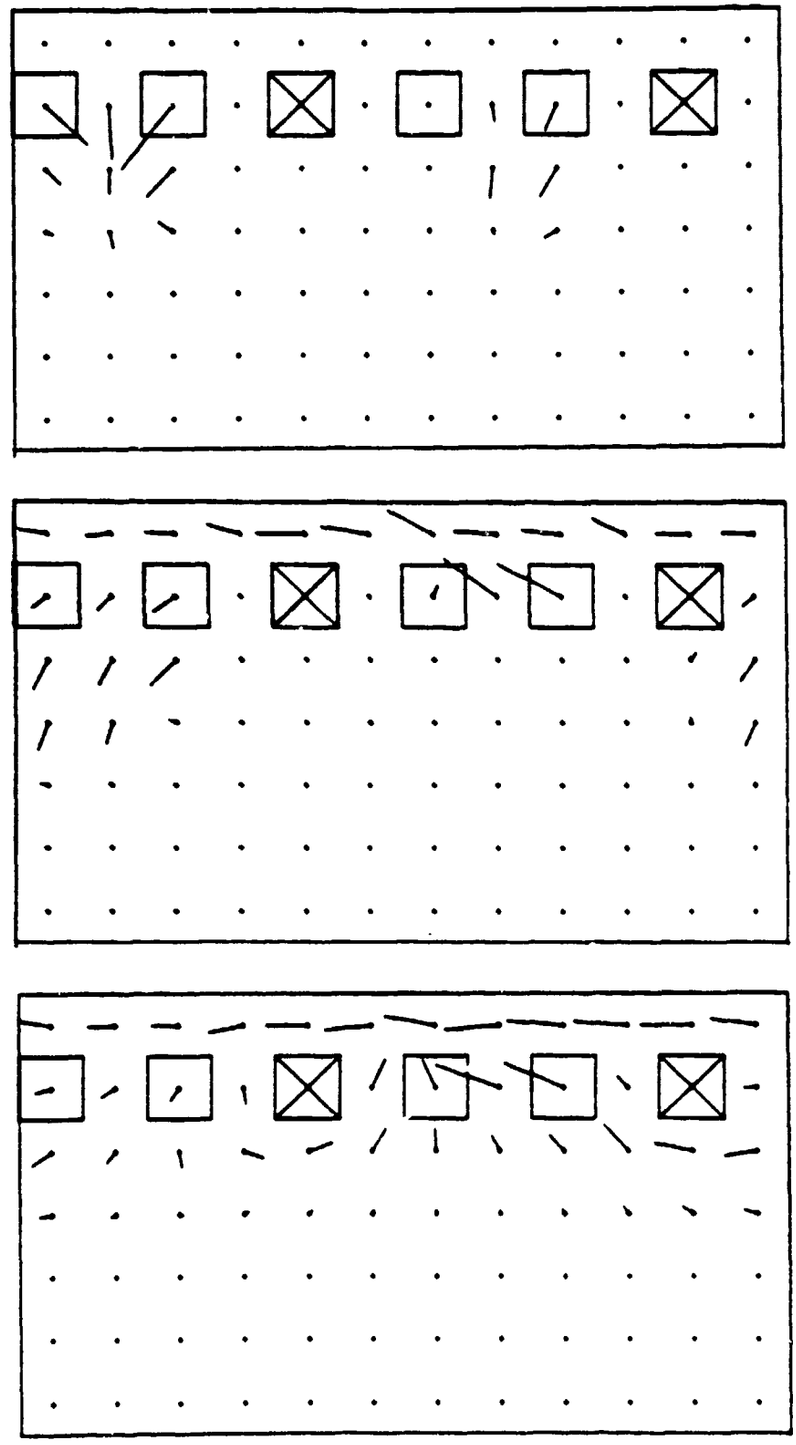

Fig. 3. Water volume flow plots showing three stages in flow development prior to the onset of water delivery to the lower plenum. Top. The injected water accumulates below the inlet legs. Middle. As a result of momentum transfer from the steam, the water is set in a swirling motion in the region above the inlet legs. Bottom. Additional momentum transfer

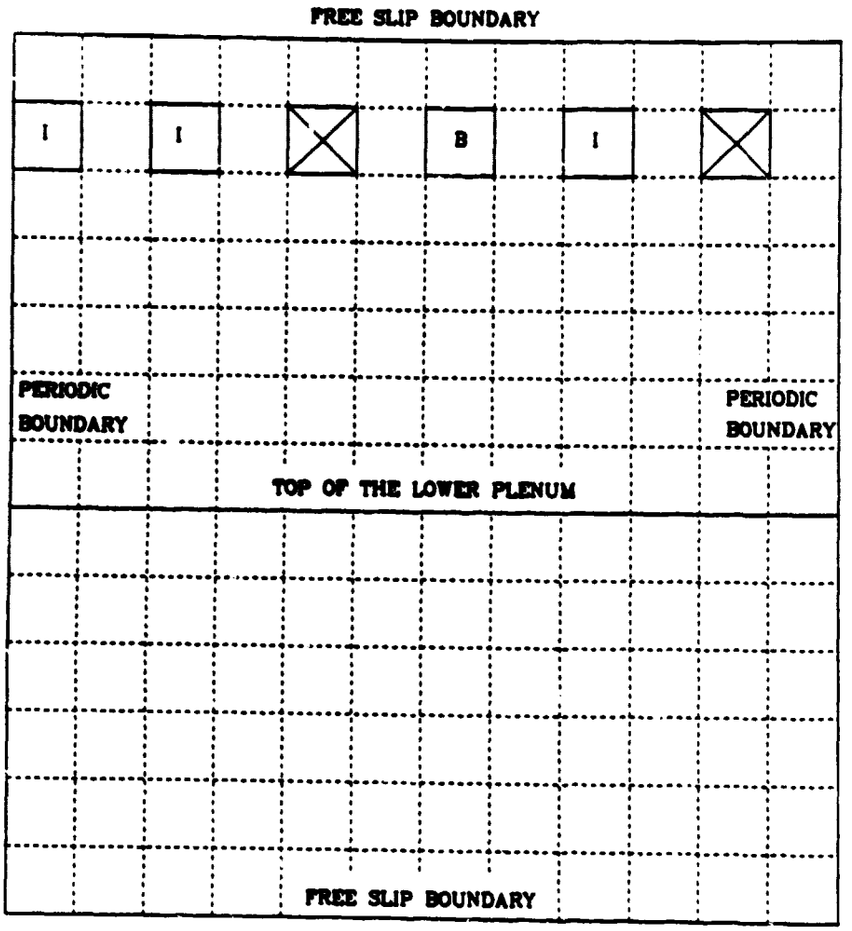

Fig. 4. Computation mesh and boundary conditions used in the transient flow comparisons at 2/15, 1/2, and full scales. In these calculations steam was injected throughout those parts of the lower plenum that were not occupied by water.

full scale are from the same calculation in all four plots. The water and steam inflow specification used in that calculation are obtained from a system calculation of a hypothetical loss of coolant accident in a full scale reactor.

The purpose of these comparisons is to determine which type of inflow specification results in small scale results that are similar to full scale in the sense described above, i.e., that have the same per cent of injected water delivered to the lower plenum when the lower plenum is 90% full, and that have reached the same stage of flow development. The latter criterion is satisfied in all cases except Fig. 6, for which the water and steam inflow velocities are proportional to scale. In that case the 2/15 scale calculation did not develop beyond the first stage of flow development, while the 1/2 scale calculation reached the second stage of development and the full scale calculation reached the third stage.

The first criterion for similarity of flow at different scales seems to be best satisfied in Fig. 8, in which the inflow velocity of the water is proportional to scale and the inflow velocity of the steam is the same at all scales. Thus at this stage of the numerical scaling study this appears to be the best type of boundary specification.

The results in Figs. 5-8 can be explained in terms of the effect that the various inflow velocity specifications have on the area of contact and the rel-

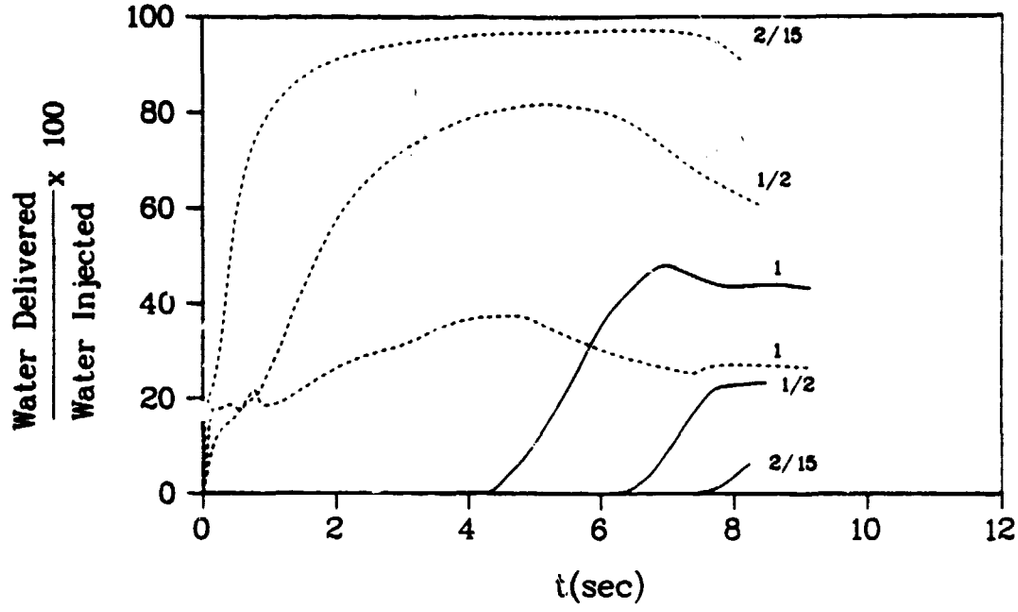

Fig. 5. Water delivered to the lower plenum (solid lines) and bypassed through the broken leg (dashed lines) as a percentage of water injected up to that time when the inflow velocities of water and steam are constant with scale. Results are shown for 2/15, 1/2, and full scale calculations.

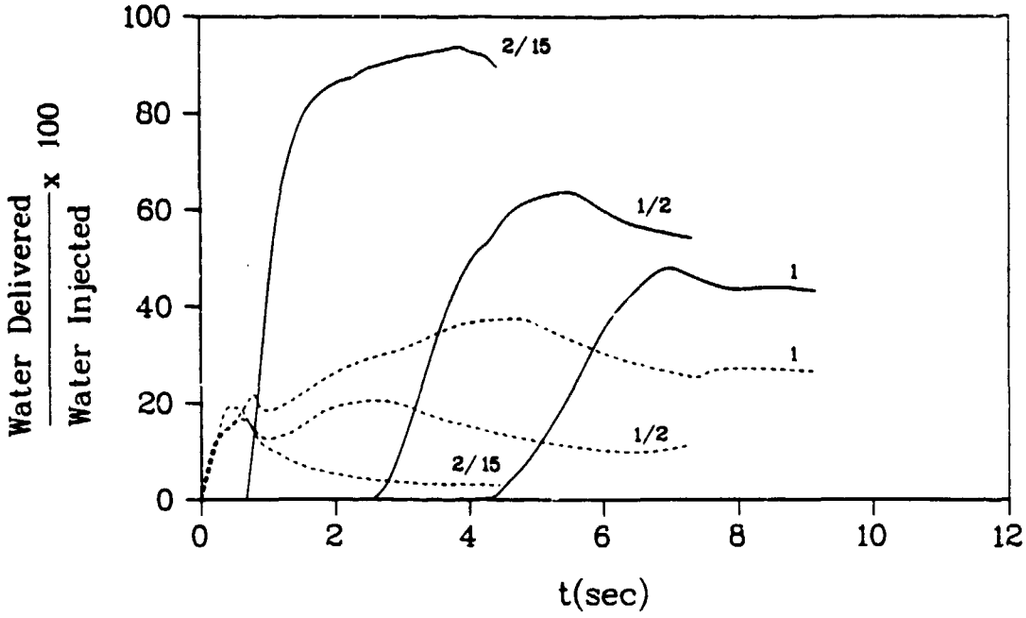

Fig. 6. Water delivered to the lower plenum (solid lines) and bypassed through the broken leg (dashed lines) as a percentage of water injected up to that time when the inflow velocities of water and steam are proportional to scale. Results are shown for 2/15, 1/2, and full scale calcula-

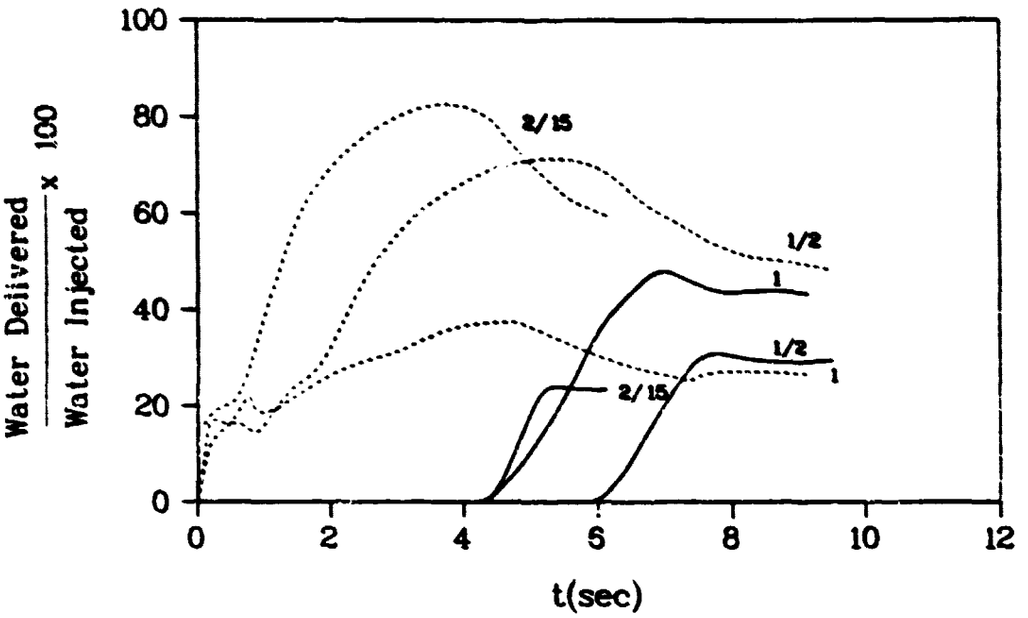

Fig. 7. Water delivered to the lower plenum (solid lines) and bypassed through the broken leg (dashed lines) as a percentage of water injected up to that time when the inflow velocities of water and steam are proportional to the square root of the scale. Results are shown for 2/15, 1/2, and full scale calculations.

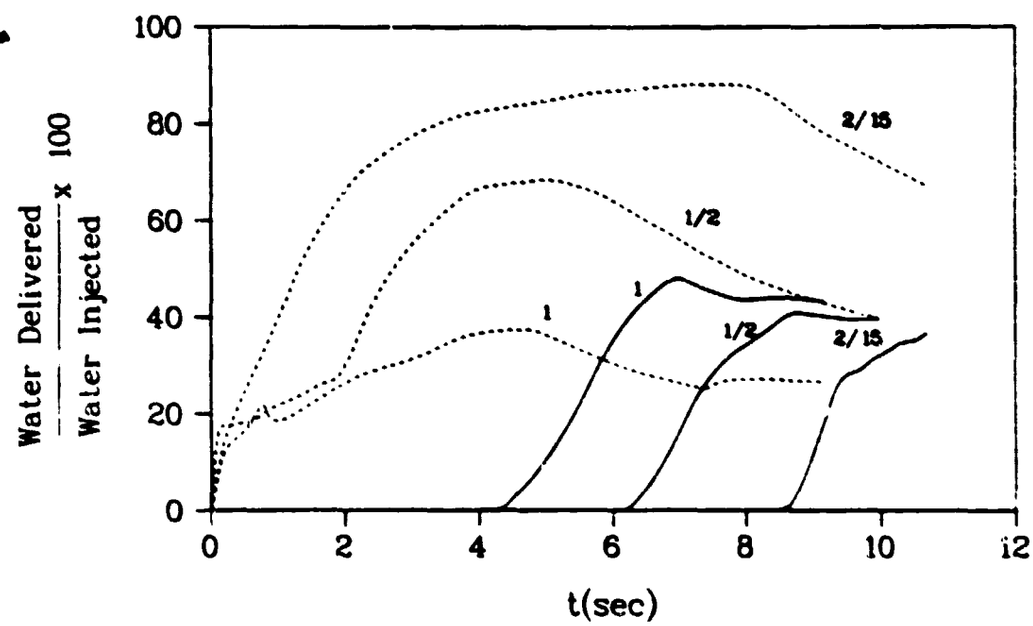

Fig. 8. Water delivered to the lower plenum (solid lines) and bypassed through the broken leg (dashed lines) as a percentage of water injected up to that time when the inflow velocity of water is proportional to scale and the inflow velocity of steam is constant with scale. Results are shown for 2/15, 1/2, and full scale calculations.

exchange. The area of contact between the fluids is influenced to a great extent by the amount of spreading of the inflowing water, and this spreading is in turn related to the local overpressure resulting from the volumetric source of water in that mesh cell. For an incompressible fluid the pressure change in a control volume is proportional to the input rate of volume per unit volume per unit time. If the inflow velocity of the water is proportional to scale, then the overpressure, the spreading and the contact interfacial area will also be proportional to scale. When the contact interface is proportional to scale, the area available for mass and momentum transfer through condensation and fluid drag will also be proportional to scale.

It is also important that the relative velocity between the phases be the same at all scales in order that the momentum transfer scale appropriately. The relative velocity within the downcomer is determined from the difference between the inflow velocities of water and steam. However, since the inflow velocity of the steam is many times that of the water, the relative velocity of flow within the downcomer is primarily determined by the inflow velocity of the steam.

Thus, similarity of flow at all scales requires that the inflow velocity of the water be proportional to scale and the inflow velocity of the steam be the same at all scales. These are the conditions that exist for the three calculations of Fig. 8, and these results show a greater similarity of flow at different scale than those of Figs. 5-7.

ACKNOWLEDGMENT

This work was supported by the U. S. Nuclear Regulatory Commission.

REFERENCES

1. Amsden, A. A. and Harlow, F. H., "K-TIF: A Two-Fluid Computer Program for Downcomer Flow Dynamics," Los Alamos Scientific Laboratory report LA-6994 (1978).

2. Harlow, F. H. and Amsden, A. A., "Flow of Interpenetrating Material Phases," J. Comp. Physics 18, 440 (1975).

3. Daly, B. J., "Nuclear Reactor Safety, Quarterly Progress Report, April 1 - June 30, 1977," LA-NUREG-6934-PR, p.22 (1977).

4. Richter, H. J. and Lovell, T. W., "The Effect of Scale on Two-Phase Countercurrent Flow Flooding in Vertical Tubes," unnumbered report from Thayer School of Engineering, Dartmouth College (1977).

5. Amsden, A. A., Daly, B. J., and Harlow, F. H., "Nuclear Reactor Safety, Quarterly Progress Report, October 1 - December 31, 1977," LA-7195-PR (1978).

6. Crowley, C. J., Block, J. A., and Cary, C. N., "Downcomer Effects in a 1/15-Scale PWR Geometry-Experimental Data Report," Creare, Inc., Hanover, NH, U. S. Nuclear Regulatory Commission report NUREG-281 (1977).

7. Carbiener, W. A., Cudnik, R. A., Dykhuizen, R. C., Denning, R. S., Flanigan, L. J., and Liu, J. S., "Steam-Water Mixing and System Hydrodynamics Program," Battelle Columbus Laboratories report BMI-NUREG-1987 (1977).